Optimization of Light Field for Generation of Vortex Knot

Song Wang(王松), Lei Wang(王磊), Furong Zhang(张福荣), and Ling-Jun Kong(孔令军)*

Key Laboratory of Advanced Optoelectronic Quantum Architecture and Measurements of Ministry of Education, Beijing Key Laboratory of Nanophotonics & Ultrafine Optoelectronic Systems, School of Physics, Beijing Institute of Technology, Beijing 100081, China

(Received 6 August 2022; accepted manuscript online 21 September 2022)

The theory of knots and links focuses on the embedding mode of one or several closed curves in three-dimensional Euclidean space. In an electromagnetic field system, all-optical knots or links composed of phase or polarization singularities have been verified theoretically and experimentally. Recent studies have shown that robust topological all-optical coding can be achieved by using optical knots and links. However, in the current design of optical knots and links based on phase or polarization singularities, the amplitude of light between adjacent singularities is relatively weak. This brings great pressure to detection of optical knots and links and limits their applications. Here, we propose a new optimization method in theory. Compared with the existing design methods, our design method improves the relative intensity distribution of light between adjacent singularities. We verify the feasibility of our design results in experiments. Our study reduces the detection difficulty of optical knots and links, and has a positive significance for promotion of applications of optical knots and links.

DOI: 10.1088/0256-307X/39/10/104101

Vortex is a common phenomenon in nature. In a complex scalar wave field, the vortex singularity is a point with uncertain phase, and intensity of the field at this point is zero. The study of optical vortex can be traced back to the study of Goos–Hänchen displacement.[1] Later, Coullet *et al.* first used the term "optical vortex" to describe laser modes that may have phase singularity.[2] In the three-dimensional space light field, the curve formed by the continuous distribution of phase singularities is called the vortex line, also known as the zero-value line in the light field. The distribution configuration of vortex lines in the three-dimensional light field is mainly divided into two categories: (1) The first one passes through the whole three-dimensional light field in an unbounded form. This vortex line extends on the central axis along the propagation direction of the light field or parallel to the axis, and its corresponding light field has a stable topology in the propagation process.[3] The research on this kind of light field mainly focuses on the spiral phase mode and the energy flow distribution in the beam.[4] For example, the most typical example is the orbital angular momentum (OAM), which has been widely studied.[5–18] (2) For the second one, the vortex line is closed in the three-dimensional light field, forming a complex knotted or linked topological structure. In mathematical language, the theory of knots and links studies the embedding mode of one or several closed curves in three-dimensional Euclidean space. In geometric topology, if two knots or links can be transformed into each other through the continuous deformation of the closed curve, these two knots or links are topologically equivalent. The topological properties of knots and links can be described by corresponding topological invariants. Because of its unique topological stability, knotted and linked structure plays an important role in research of physics and life science. At present, knots and links have been observed in plasma,[19] quantum and classical fluids,[19] quantum and classical field theory,[20–23] liquid crystal,[24,25] sound wave,[26] and optical fields.[27–34] Recent investigations have also shown that optical framed knots and links can be used in conjunction with prime factorization to encode information.[35] Due to robustness of topological light fields, such a coding scheme has good stability against external perturbations. The optical knot or link is reconstructed by detecting and connecting the intensity singularities, which are contained in a series of two-dimensional intensity distribution planes along the direction of beam propagation. Therefore, when designing and constructing a three-dimensional optical knot or link, there is a high requirement for the contrast between the phase vortices (phase singularities). How to accurately determine the position of the singularities plays a vital role in reconstruction of optical knot or link. However, when using modal superposition to construct isolated vortex knot or link, the vortex lines are intertwined in the region of very low light intensity. This makes it difficult to accurately reconstruct them. More importantly, in the current optical knot or link design based on phase or polarization singularity, the intensity of light between adjacent vortex singularities is relatively weak, which makes it more difficult to detect the optical knots and links.

In this Letter, we propose an optimization by adjusting the parameter of coefficient of overhomogenization. Compared with the existing design methods, our design results improve the relative intensity distribution of light between adjacent singularities. We verify the feasibility of our design results in experiments. Our study greatly reduces the

*Corresponding author. Email: konglj@bit.edu.cn
© 2022 Chinese Physical Society and IOP Publishing Ltd

detection difficulty of optical knots and links, and has a positive significance for promotion of applications of optical knots and links.

The theory of knot and link has been extensively studied before. It has been realized that the abstract function with knotted or linked zeroes could be constructed by devising complex functions on a periodic braid embedded in a cylinder.[29,35] In the braid representation (x', y', h), the braid is composed of some twined strands. The intersection of horizontal two-dimensional horizontal plane (x', y') and strands will rotate periodically with the change of parameter h. The general expression of the braid structure corresponding to the constructed knot or link is

$$x'^{s,r}_j(h) = \cos\Big(\frac{1}{s}[rh + 2\pi(j-1)]\Big),$$
$$y'^{s,r}_j(h) = \sin\Big(\frac{1}{s}[rh + 2\pi(j-1)]\Big), \quad (1)$$

where r is the number of basic cycles, s is the total number of strands in the braid, $j = 1, 2, \ldots, s$. In the three-dimensional space (x', y', h), these strands are the curves $S^{s,r}_j(h)$:

$$S^{s,r}_j(h) = (x'^{s,r}_j(h), y'^{s,r}_j(h), h). \quad (2)$$

Here, $0 \leqslant h \leqslant 2\pi$. When $r = 3$, $s = 2$, the form of braid is shown in Fig. 1(a). By introducing the complex coordinates (u, v) as $u = x' + iy'$ and $\nu = e^{ih}$, the strands can be expressed as roots of a complex polynomials given as follows:

$$q^{s,r}(u, v) = \prod_{j=1}^{s}(u - \nu^{r/s} e^{i2\pi(j-1)/s}). \quad (3)$$

Then, based on a stereographic projection,[29,35] the polynomial $q(u, v)$ can be converted into a complex field in the (x, y, z) coordinate system as

$$f^{s,r}(x, y, z) = \prod_{j=1}^{s}\Big(\frac{R^2 + (z+i)^2}{R^2 + z^2 + 1} - \Big(\frac{2Re^{i\vartheta}}{R^2 + z^2 + 1}\Big)^{r/s} e^{i2\pi(j-1)/s}\Big). \quad (4)$$

Here, $R = \sqrt{x^2 + y^2}$, ϑ represents the rotational coordinate in a (x, y, z) coordinate system. The $f^{s,r}(x, y, z)$ is called the Milnor polynomial, which contains the knotted or linked zero-value lines. When $r = 3$, $s = 2$, $j = 1, 2$, the corresponding Milnor polynomial of the braid in Fig. 1(a) is

$$f_{\text{trefoil}}(x, y, z) = \Big[\frac{R^2 + (z+i)^2}{R^2 + z^2 + 1}\Big]^2 - \Big(\frac{2Re^{i\vartheta}}{R^2 + z^2 + 1}\Big)^3. \quad (5)$$

The zero-line contained in $f_{\text{trefoil}}(x, y, z)$ is shown in Fig. 1(b), which is a trefoil knot. As pointed out in Ref. [29], the Milnor polynomial diverges as $x, y \to \infty$, and it cannot be used to represent the complex amplitude of the light field directly. The correct knot occurs by evolving the field:

$$\psi_{\text{kont}}(x, y, z = 0) = f(x, y, z = 0)(R^2 + 1)^n e^{-R^2/\omega^2}. \quad (6)$$

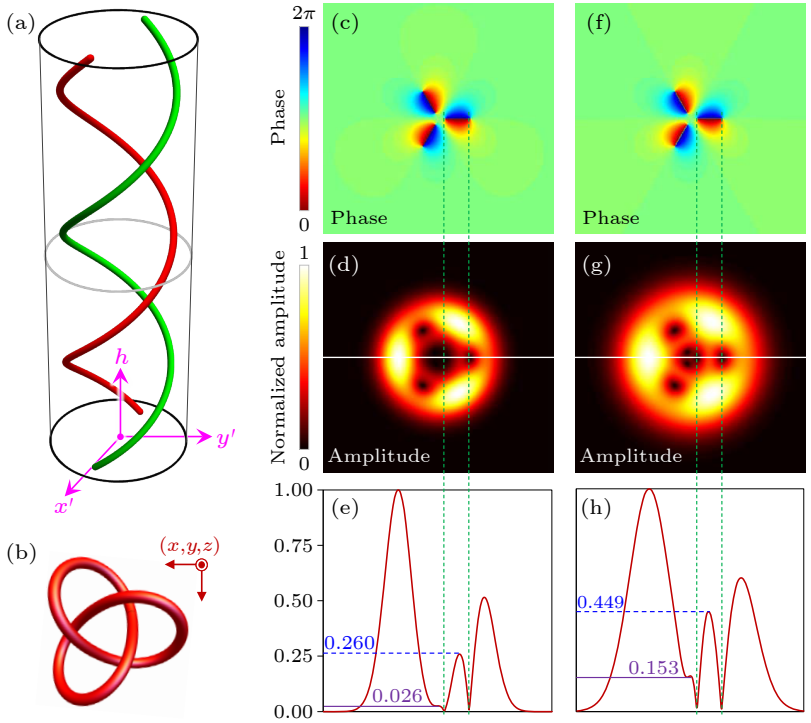

Fig. 1. (a) The braid representation of trefoil knot in (x', y', h). (b) The three-dimensional topological structure of trefoil knot. (c) and (d) The phase distribution $\arg[\psi_{\text{trefoil}}(x, y, z = 0)]$ and amplitude distribution $|\psi_{\text{trefoil}}(x, y, z = 0)|$ for generating optical trefoil knot before optimization, respectively. (e) The amplitude distribution along the white line in (d). (f) and (g) The phase distribution $\arg[\psi_{\text{trefoil}}(x, y, z = 0)]$ and amplitude distribution $|\psi_{\text{trefoil}}(x, y, z = 0)|$ for generating optical trefoil knot after optimization, respectively. (h) The amplitude distribution along the white line in (g).

The process of multiplying $f(x, y, z = 0)$ by sufficiently large powers of $(R^2 + 1)^n$ is called the "overhomogenization".[36] In the previous work, the coefficient of overhomogenization (n) is set to be equal to the number of basic cycles (r). For example, in the case of trefoil knot, $n = 3$. According to Eq. (6), the phase distribution $\arg[\psi_{\text{trefoil}}(x, y, z = 0)]$ and amplitude distribution $|\psi_{\text{trefoil}}(x, y, z = 0)|$ for generating optical trefoil knot can be obtained as shown in Figs. 1(c) and 1(d), respectively. Here, the parameter $\omega = 1.2$. It can be seen clearly from Fig. 1(c) that there are six phase singularities appeared. Accordingly, Fig. 1(d) contains six singularities with amplitude 0, but the amplitude singularities are not obvious, especially the three in the central area. Along the direction of beam propagation, the number and relative position of singularities will change. By connecting the singularities in turn along the propagation direction, the topological structure of the knot can be reconstructed. Therefore, the detection of the number and relative position of singularities at different propagation positions is the key to reconstructing the topological structure of knot experimentally. However, as shown in Fig. 1(d), the light field amplitude distribution between the six amplitude singularities is relatively small. Figure 1(e) shows the amplitude distribution along the white line in Fig. 1(d). It can be seen from Fig. 1(e) that the minimum of the relative amplitudes among the singularities in the central region is only 0.026, and the relative amplitude between peripheral and central singularities is only 0.246. This makes it difficult to accurately locate them. If the amplitude distribution of the required light field can be optimized and the relative amplitude between adjacent singularities can be increased, the difficulty of optical knot detection can be greatly reduced.

It can be seen from Eq. (6) that the complex amplitude $\psi_{\text{kont}}(x, y)$ is not only the function of the horizontal coordinate (x, y), but also affected by the parameter ω and the coefficient of overhomogenization n. Therefore, here we consider these two parameters at the same time to optimize the complex amplitude distribution $\psi_{\text{kont}}(x, y)$. Our optimization results show that when $\omega = 1.75$ and the coefficient of overhomogenization $n = 1.5$, the light field phase distribution $\arg[\psi_{\text{trefoil}}(x, y, z = 0)]$ and the amplitude distribution $|\psi_{\text{trefoil}}(x, y, z = 0)|$ are calculated with Eq. (6), as shown in Figs. 1(f) and 1(g). Figure 1(h) shows the amplitude distribution along the white line in Fig. 1(g). It can be seen from Fig. 1(h) that, after optimization, the minimum of the relative amplitudes among the three central singularities is increased to 0.153, which is about 6 times that before optimization. The relative amplitude between peripheral and central singularity is increased to 0.449, about twice the value before optimization.

To verify the feasibility of our optimization method, we have experimentally created the isolated optical vortex knots and links. The experimental setup is shown in Fig. 2(a). The incident beam, which is a monochromatic polarized light beam with wavelength $\lambda = 633\,\text{nm}$, is manipulated to illuminate the spatial light modulator (SLM). The modulated beam then passes through a $4f$ system, which consists of two lenses (lens 1 and lens 2) and a filter located at the back focal plane of the Lens1. In this case, only the first-order diffracted beam could be imaged on the back focal plane of lens 2. Such an image plane is defined as the $z = 0$ plane, which corresponds to the central plane of light fields sustaining vortex knots and links. A CCD camera is used to measure the intensity profile of the light field. The CCD is placed on a translation stage (along the z-direction), allowing a full 3D scan of the transmitted beam and finding the precise locations of the amplitude singularities of the vortex lines. About 100 such planes are measured, allowing the vortex configuration in the volume to be determined precisely. Figure 2(b) shows the amplitude distribution at the plane of $z = 0$. Clearly, there are six amplitude singularities. Figure 2(c) shows the amplitude distribution along the white line in Fig. 2(b). It can be seen from Fig. 2(c) that in the normalized amplitude distribution detected in the experiment, the minimum of the relative amplitudes among the three central singularities is about 0.122, and the maximum of the relative amplitude between the peripheral and central singularities is about 0.460. The experimental results agree with the theoretical ones. Figure 2(d) shows the trefoil knot measured in experiment.

To prove the universality of our optimization method, we have also constructed the cinquefoil knot and compared it with the one obtained in the previous work.[35,37] The normalized amplitude distribution $|\psi_{\text{cinquefoil}}(x, y, z = 0)|$ used to generate the optical cinquefoil knot is shown in Fig. 3(a). There are ten singularities, but the singularities are not obvious, especially the five in the central region. Figure 3(b) shows the amplitude distribution along the white line in Fig. 3(a). The minimum of the relative amplitudes among the five central singularities is only 0.040. The maximum of the relative amplitude between the peripheral and central singularities is only 0.206. This low contrast will bring great difficulties to accurately locate them.

Next, we will optimize this complex amplitude distribution of the light field by setting the parameter $\omega = 1$ and the coefficient of overhomogenization $n = 2.5$. After optimization, the normalized amplitude distribution used to generate optical cinquefoil knot is shown in Fig. 3(c). Figure 3(d) shows the amplitude distribution along the white line in Fig. 3(c). It can be seen from Fig. 3(d) that, in the optimized amplitude distribution, the minimum of the relative amplitudes among the five singularities in the central area has been increased to 0.077. The relative amplitude between the peripheral and central singularities has been increased to 0.544. In experiment, we directly detect the intensity distribution along the direction of propagation of the light field. About 100 such planes are measured, allowing the vortex configuration in the volume to be determined precisely. Then the positions of the amplitude singularities are located and connected. Figure 3(e) presents the experimental result of Fig. 3(c). Figure 3(f) shows the amplitude distribution along the white line in Fig. 3(e). It can be seen from Fig. 3(e) that, in the normalized amplitude distribution detected in the experiment, the minimum of the relative amplitudes among the five singularities in the center is about 0.045, and the relative amplitude between the peripheral and central singularities is about 0.521. The experimental results are ba-

sically consistent with the theoretical results. Figure 3(g) shows the three-dimensional cinquefoil knotted structure reconstructed in experiment. It should be pointed out that there are small deviations between our experimental results shown in Fig. 2(c) [Fig. 3(f)] and the theoretical results shown in Fig. 1(h) [Fig. 3(d)]. These deviations mainly come from the imperfection of the alignment of optical elements and modulation function of the SLM. The environment in the laboratory and the detector will also introduce some noise.

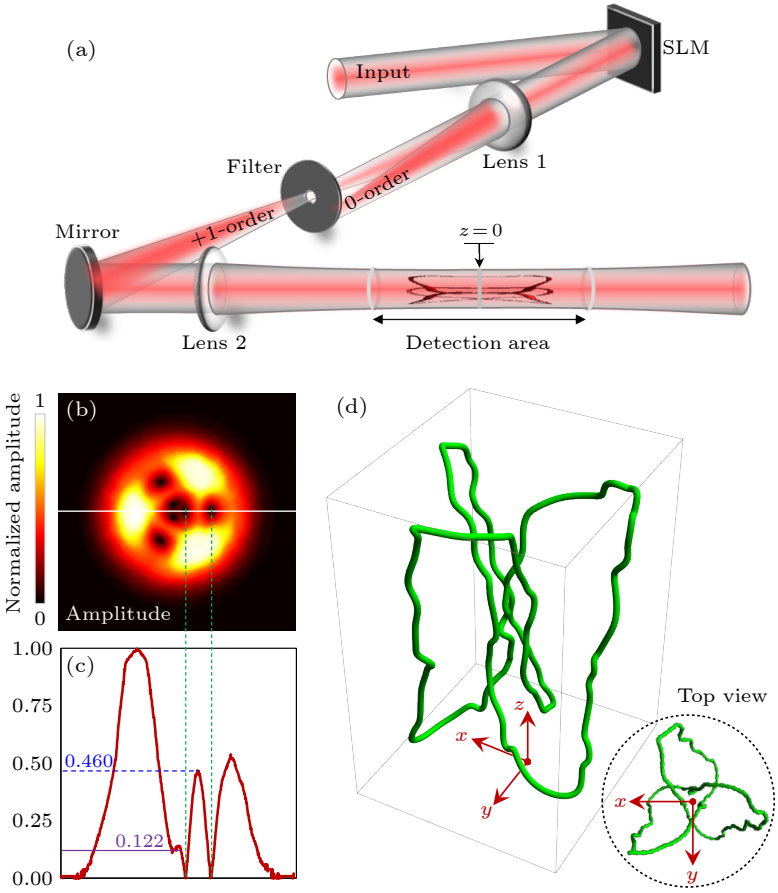

Fig. 2. (a) Experimental apparatus used to generate vortex knots and links. The incident multi-wavelength light field consists of three different wavelengths (633 nm). The SLM is placed on the front focal plane of the $4f$ system, which consists of lenses 1 and 2. A filter on the back focal plane of lens 1 filters out the light unwanted. The knots and links can be reconstructed by measuring the intensity distribution in the detection area with a CCD (not shown). (b) Normalized amplitude distribution after optimization measured in the experiment. (c) The amplitude distribution along the white line in (b). (d) The topological structure of the trefoil knot reconstructed in experiment. The inset shows a top view of the trefoil knot.

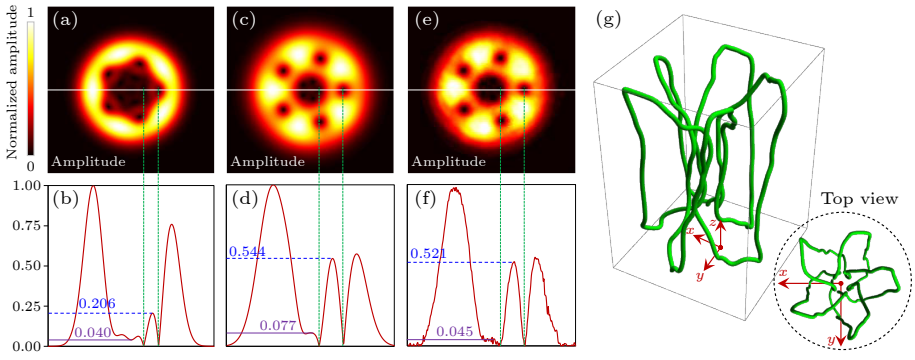

Fig. 3. (a) The amplitude distribution for generating optical cinquefoil knot before optimization. (b) The amplitude distribution along the white line in (a). (c) The amplitude distribution for generating optical cinquefoil knot after optimization. (d) The amplitude distribution along the white line in (c). (e) The experimental result corresponding to (c). (f) The amplitude distribution along the white line in (e). (g) The topological structure of the cinquefoil knot reconstructed in the experiment. The set shows a top view of the cinquefoil knot.

In order to reduce the difficulty of detecting amplitude singularities in the reconstruction of the knotted and linked structures, interferometers have been used to transform the amplitude singularities into phase singularities.[38] In this method, the difficulty of accurately locating of phase singularity depends on the contrast of interference fringes. While the contrast of interference fringes (especially near the singularities) depends on the relative amplitude distribution of light field between adjacent singularities, improving the relative amplitude distribution of light field between adjacent singularities is also very important for reducing the difficulty of accurately locating the singularities in the method with interferometers.

In summary, based on the knots and links structure theory, we have proposed and implemented an optimization method to generate isolated optical vortex knots and links by breaking the limitation that the coefficient of overhomogenization can only be taken as a positive integer. Compared with the existing design methods, our method improves the relative amplitude distribution of light field between adjacent singularities and greatly reduces the difficulty of accurately locating the singularities. For the trefoil knot, after optimization, the minimum of the relative amplitudes among the three singularities in the center area has been increased to 0.153, which is about 6 times the value before optimization. The relative amplitude between the peripheral and central singularities has been increased to 0.449, about twice the value before optimization. For the cinquefoil knot, similar results have been obtained, which prove the universality of our method. We have also experimentally verified the feasibility of our design results, and the experimental results are consistent with the theoretical results. Our study has greatly reduced the difficulty of detecting optical knots and links, and has a positive significance for promotion of applications of optical knots and links.

Acknowledgments. This work was supported by the National Key R&D Program of China (Grant No. 2017YFA0303800), and the National Natural Science Foundation of China (Grant No. 12004038).

References

[1] Dennis M R, O'Holleran K, and Padgett M J 2009 *Singular Optics: Optical Vortices and Polarization Singularities* in *Progress in Optics* (Amerstam: Elsevier) vol 53 chap 5 p 293
[2] Coullet P, Gil L, and Rocca F 1989 *Opt. Commun.* **73** 403
[3] Li P, Guo X, Zhong J, Liu S, Zhang Y, Wei B, and Zhao J 2021 *Adv. Phys.: X* **6** 1843535
[4] O'Neil A T, MacVicar I, Allen L, and Padgett M J 2002 *Phys. Rev. Lett.* **88** 053601
[5] Allen L, Beijersbergen M W, Spreeuw R J C, and Woerdman J P 1992 *Phys. Rev. A* **45** 8185
[6] Mair A, Vaziri A, Weihs G, and Zeilinger A 2001 *Nature* **412** 313
[7] Kong L J, Qian S X, Ren Z C, Wang X L, and Wang H T 2012 *Phys. Rev. A* **85** 035804
[8] Jack B, Leach J, Romero J, Franke-Arnold S, Ritsch-Marte M, Barnett S M, and Padgett M J 2009 *Phys. Rev. Lett.* **103** 083602
[9] Wang J *et al.* 2012 *Nat. Photon.* **6** 488
[10] Devlin R C, Ambrosio A, Rubin N A, Mueller J P B, and Capasso F 2017 *Science* **358** 896
[11] Zeng Q, Wang B, Li P, and Zhang X 2018 *Phys. Rev. Lett.* **120** 030401
[12] Kong L J, Liu R, Qi W R, Wang Z X, Huang S Y, Wang Q, Tu C, Li Y, and Wang H T 2019 *Sci. Adv.* **5** eaat9206
[13] Brullot W, Vanbel M K, Swusten T, and Verbiest T 2016 *Sci. Adv.* **2** e1501349
[14] Kong L J, Liu R, Qi W R, Wang Z X, Huang S Y, Tu C, Li Y, and Wang H T 2020 *Chin. Phys. Lett.* **37** 034204
[15] Fang X, Yang H, Yao W, Wang T, Zhang Y, Gu M, and Xiao M 2021 *Adv. Photon.* **3** 015001
[16] Cai X, Wang J, Strain M J, Johnson-Morris B, Zhu J, Sorel M, O'Brien J L, Thompson M G, and Yu S 2012 *Science* **338** 363
[17] Padgett M and Bowman R 2011 *Nat. Photon.* **5** 343
[18] Kozawa Y, Matsunaga D, and Sato S 2018 *Optica* **5** 86
[19] Moffatt H K 1969 *J. Fluid Mech.* **35** 117
[20] Faddeev L and Niemi A J 1997 *Nature* **387** 58
[21] Battye R A and Sutcliffe P M 1998 *Phys. Rev. Lett.* **81** 4798
[22] Matthews M R, Anderson B P, Haljan P C, Hall D S, Wieman C E, and Cornell E A 1999 *Phys. Rev. Lett.* **83** 2498
[23] Ruostekoski J and Dutton Z 2005 *Phys. Rev. A* **72** 063626
[24] Martinez A, Ravnik M, Lucero B, Visvanathan R, Žumer S, and Smalyukh I I 2014 *Nat. Mater.* **13** 258
[25] Machon T and Alexander G P 2014 *Phys. Rev. Lett.* **113** 027801
[26] Zhang H, Zhang W, Liao Y, Zhou X, Li J, Hu G, and Zhang X 2020 *Nat. Commun.* **11** 3956
[27] Leach J, Dennis M R, Courtial J, and Padgett M J 2004 *Nature* **432** 165
[28] Irvine W T M and Bouwmeester D 2008 *Nat. Phys.* **4** 716
[29] Dennis M R, King R P, Jack B, O'Holleran K, and Padgett M J 2010 *Nat. Phys.* **6** 118
[30] Pisanty E, Machado G J, Vicuña-Hernández V, Picón A, Celi A, Torres J P, and Lewenstein M 2019 *Nat. Photon.* **13** 569
[31] Leach J, Dennis M R, Courtial J, and Padgett M J 2005 *New J. Phys.* **7** 55
[32] Maucher F, Skupin S, Gardiner S A, and Hughes I G 2018 *Phys. Rev. Lett.* **120** 163903
[33] Romero J, Leach J, Jack B, Dennis M R, Franke-Arnold S, Barnett S M, and Padgett M J 2011 *Phys. Rev. Lett.* **106** 100407
[34] Kong L J, Zhang W, Li P, Guo X, Zhang J, Zhang F, Zhao J, and Zhang X 2022 *Nat. Commun.* **13** 2705
[35] Larocque H, D'Errico A, Ferrer-Garcia M F, Carmi A, Cohen E, and Karimi E 2020 *Nat. Commun.* **11** 5119
[36] Bode B, Dennis M R, Foster D, and King R P 2017 *Proc. R. Soc. A* **473** 20160829
[37] Larocque H, Sugic D, Mortimer D, Taylor A J, Fickler R, Boyd R W, Dennis M R, and Karimi E 2018 *Nat. Phys.* **14** 1079
[38] Guo X, Li P, Zhong J, Liu S, Wei B, Zhu W, Qi S, Cheng H, and Zhao J 2020 *Laser & Photon. Rev.* **14** 1900366